Journal of Innovative Materials in Extreme Conditions
2020
Volume 1
Issue 1

LUMINESCENCE PROPERTIES OF Eu^{3+} DOPED MAYENITE UNDER HIGH PRESSURE

B. Matovic[1*], M. Nikolic[2], M. Prekajski Djordjevic[1], S. Dmitrovic[1], J. Lukovic[1], J. Maletaskic[1], B. Jelenkovic[2]

[1]Center for synthesis, processing, and characterization of materials for application in the extreme conditions "CextremeLab", VINCA Institute of Nuclear Sciences - National Institute of the Republic of Serbia, University of Belgrade, Belgrade, Serbia
[2]Institute for Physics, Belgrade University, Belgrade, Serbia
Corresponding author: mato@vinca.rs*

Abstract: *Europium doped mayenite ($C_{12}A_7$) powders of different concentrations (0.5, 1.0, 1.5, and 2.0 at.%) have been synthesized by a modified glycine/nitrate procedure - MGNP). Obtained samples were characterized by X-ray diffraction (XRD), field emission scanning electron microscopy (FE-SEM), and steady-state photoluminescence spectroscopy. The effect of doping concentration on photoluminescence properties of Eu^{3+} doped mayenite was studied and discussed. With the increasing of Eu^{3+} doping concentration, the red-emitting intensity exhibited behavior that increased firstly and then decreased. The optimal Eu^{3+} ion concentration is found to be 1.5%. High-pressure luminescence was measured in a Betsa high-pressure membrane diamond anvil cell up to 23 GPa.*

1. Introduction

Mineral mayenite is one of the intermediary phases of the $CaO\text{-}Al_2O_3$ binary system, known as a constituent of calcium aluminate cement with a formula written as $12CaO{\cdot}7Al_2O_3$ or $C_{12}A_7$ in the cement-chemist notation. The first time it was originally reported from Eifel volcanic complex in Germany and is named after the place of its discovery, Mayen (Germany) by Hentschel [1]. Recently, mayenite encouraged research interest because of its oxygen mobility [2], ionic conductivity [3], high anti-carbon and anti-sulfur characteristics [4-7] and catalytic properties [8]. Mayenite possesses a distinct feature related to its crystal structure. The unit cell of $C_{12}A_7$ contains two molecules and could be expressed as a positively charged lattice framework $[(Ca_{24}Al_{28}O_{64})^{4+}]$ and $2O^{2-}$ negative one [9]. The positive part of the framework consists of three-dimensional 12 crystallographic cages per unit cell, which are interconnected in such a way that the channels of complex shape form between them with an inner free space of ~0.4 nm in diameter. The letter part, $2O^{2-}$, is known as "extra-framework oxide ions," which are distributed within the cages to maintain charge neutrality [10, 11]. It is assumed [2] that weakly bound oxygen anions can move through empty channels between cages and thereby create high oxygen conductivity in the material. Mayenite has been synthesized using various methods. The commonly used method is a solid-state reaction between $CaCO_3$ and $\gamma\text{-}Al_2O_3$ [12]. Although it is a simple way that also provides mass production, the high firing temperature is a critical issue, and a new fabrication method was developed which is also capable of being utilized at a much lower temperature. Single crystals of $C_{12}A_7$ with regular morphologies can be obtained by applying the Czochralski method [13] and floating zone (Fz) methods [14,15]. Also, a low-temperature approach is possible, such as hydrothermal and sol-gel synthesis [16,17] and oxalate precursor route [18]. One of the most efficient and precise methods is a modified glycine/nitrate procedure [19], which is used in this paper.

Since they share common planes in cages that are open and oxygen can move easily, it is assumed that the $C_{12}A_7$ structure is very sensitive to pressure. Moreover, in phosphors doped mayenite, the change can be followed by its luminescence properties due to subatomic motions or stress on a crystal. In this work, the results on synthesis and high-pressure dependent photoluminescence properties of Eu doped $C_{12}A_7$ powders are described.

2. Experimental

Precursors used for the production of the powder were Ca and Al nitrates, and Al and Ca acetate, (Aldrich, USA), and aminoacteic acid-glycine, (Fischer Scientific, USA). Europium is added as Eu nitrate in different concentrations (0.5, 1.0, 1.5, and 2.0 at.%) in order to obtain a solid solution in small concentrations. Starting chemical reactants were dissolved in a glass beaker according to the composition of $C_{12}A_7$, following thermal treatment on a hot plate until the reaction smoke is terminated. This reaction is based on self-combustion of the metal nitrate/acetate and glycine mixture which occurs at 180°C spontaneously and terminates rapidly [19]. The resulting powder was calcined to 600°C to burn any organic residues from precursors and at 1200°C to induces crystallization.
The phases of samples were identified using X-ray powder diffraction (XRPD) on an Ultima IV Rigaku diffractometer using $Cu_{K\alpha}$ radiation with a scanning step size of 0.02° and at a scan rate of 2 °/min. (2θ-range: 20 - 80°). Phase analysis was done by using the PDXL2 software (version 2.0.3.0) [20], regarding the patterns of the International Centre for Diffraction Data database (ICDD) [21], version 2018. The microstructural observations of obtained powders were performed by scanning electron microscopy (SEM), Vega Tescan.

The photoluminescence spectra measurements were done under continuous Nd YAG laser excitation at 532 nm. Data were collected from Ocean Optics USB2000 (200-800 nm) spectrometer. High-pressure luminescence was measured in a Betsa high-pressure membrane diamond anvil cell with steel gasket (T301). The sample chamber was 125 μm in diameter and 70 μm in thickness. A mixture of methanol and ethanol with a 4:1 volume ratio was selected as the pressure-transmitting medium. Ruby loaded with sample determines the pressure. For measuring Ruby R1 line shift HR2000 Ocean Optics spectrometer (600-800 nm) was used.

3. Results and discussion

The microstructure of synthesized powders exhibited a porous structure (Figure 1a). Since the reaction for $C_{12}A_7$ synthesis is based on self-combustion of the metal nitrate/acetate and glycine mixture which produced a huge amount of gaseous; normally, the highly porous texture is obtained. On the other side, the microstructure is changed after thermal treatment. Morphologies of calcined powders at 1200°C are cemented in a form of agglomerated, mostly well-formed faceted grains. Agglomerates manifested layer structure with plate grains consisting of regular crystals of a narrow size range of 0.8–1 μm and thickness roughly estimated about 200-250 nm (Figure 1b).

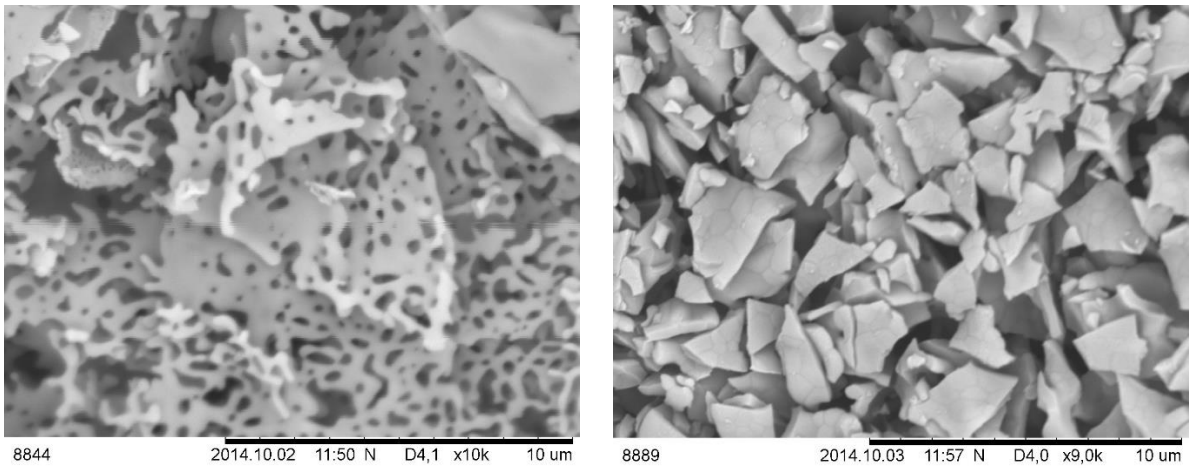

a) b)

Figure 1. SEM images of samples $C_{12}A_7$ calcinated at (a) 600°C, and at (b) 1200°C.

The XRD study confirms the SEM results. The patterns of obtained powders by the MGNP method calcined at 600°C show typical amorphous diffraction lines (Figure 2).

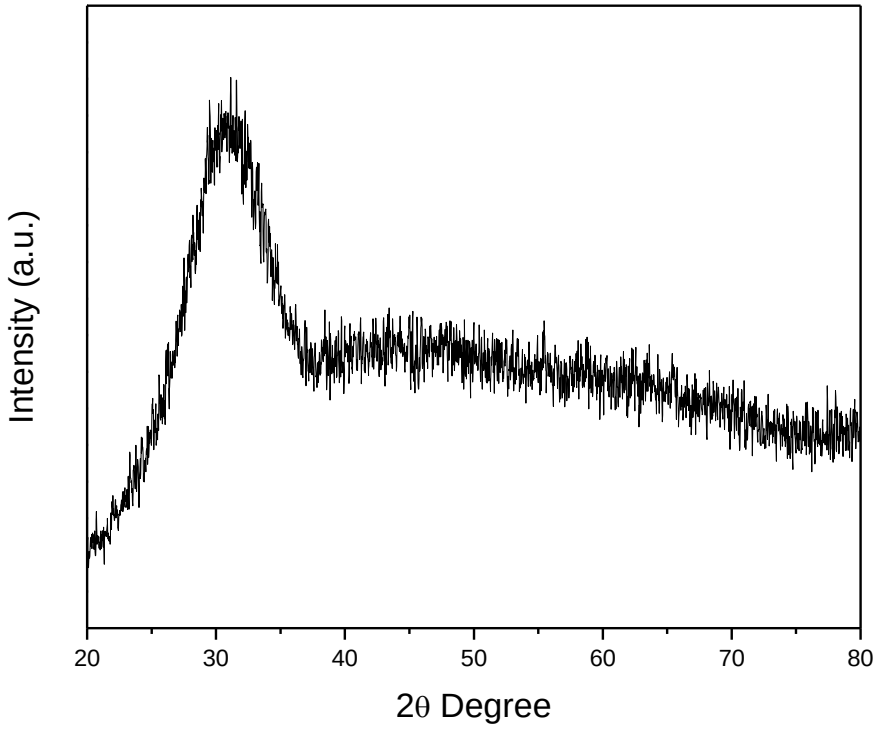

Figure 2. X-ray diffraction patterns of the powder obtained by the MGNP and calcinated at 600° /1 h.

Unlike as-synthesized powder (Figure 2), the annealed powders exhibit clear diffraction lines that could be assigned to the cubic unite cell (SG *I*-43*d* with lattice parameter a = 11.989 Å, Z = 2; JCPDS: 48-1882). Peaks relating impurities or other Ca or Al-oxide phases were not observed (Figure 3). XRD patterns of obtained $C_{12}A_7$:Eu^{3+} powders with different doping concentrations are shown in Figure3.

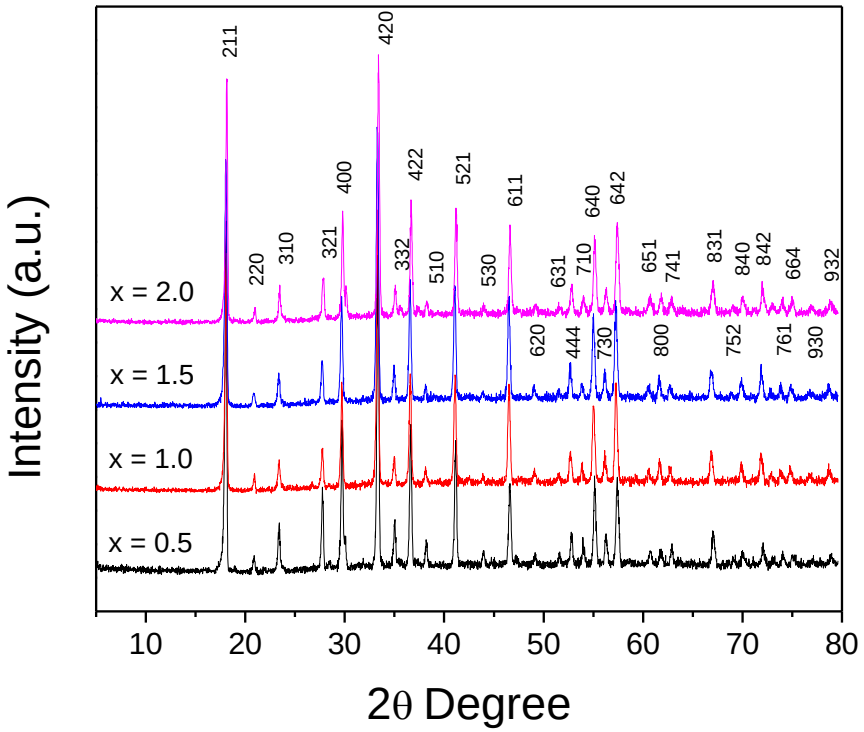

Figure 3. XRD patterns of $12CaO{\cdot}7Al_2O_3$:x% Eu^{3+} (x = 0.5; 1.0; 1.5; .2.0) calcined at 1200°C/2 h.

Emission spectra of 0.15 Eu^{3+} doped mayenite sample excited with 532 lasers are shown in Figure 4.a. In this picture, five bands associated with $^5D_0$ -^7F_J (J=4, 3, 2, 1, and 0) spin forbidden f–*f* transitions can be observed (Figure 4.b). For the $^5D_0$ -^7F_J transition we observe only one peak, which is expected knowing that the coordination difference between two Ca^{2+} non-equivalent crystallographic sites, where Eu^{3+} ion can be placed, is practically negligible.

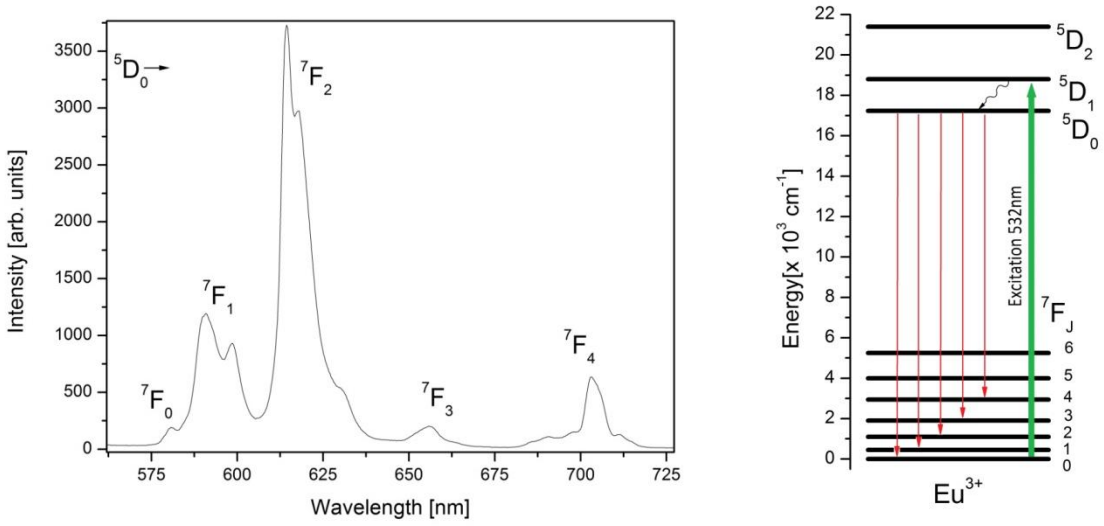

a) b)

Figure 4. a) Emission spectrum Eu^{3+} doped mayenite with 532 nm laser excitation. **b)** Energy scheme levels of Eu^{3+}

Pressure dependence of emission spectrum Eu^{3+} doped mayenite is shown in Figure 5a. The $^5D_0$-$^7F_2$ is an electric dipole transition (ΔJ=2) very sensitive to the local environment around Eu^{3+}, and its intensity depends on the symmetry of the crystal field around the europium ion. In contrast, the $^5D_0$-$^7F_1$ transition is the parity allowed magnetic dipole transition (ΔJ=1), and its intensity does not vary with the host.

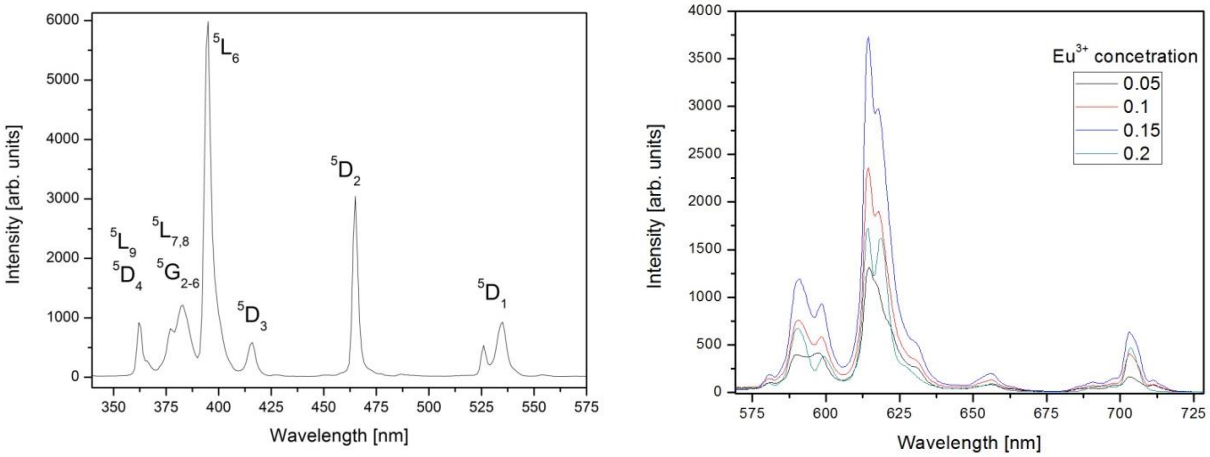

a) b)

Figure 5. **a)** Excitation spectrum Eu^{3+} doped mayenite; b**)** emission spectra of Eu^{3+} doped mayenite samples obtained with different Eu^{3+} concentrations.

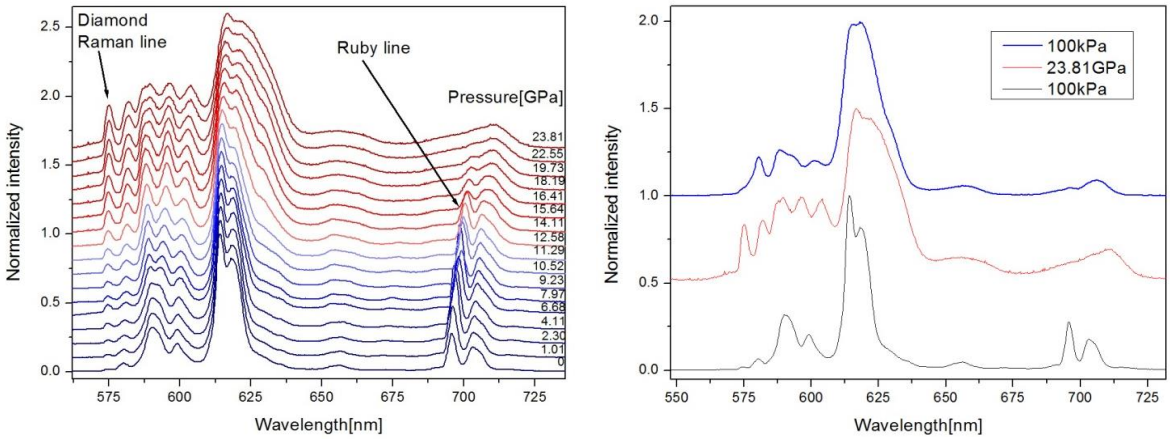

a) b)

Figure 6. a) Pressure dependence of emission spectrum Eu^{3+} doped mayenite. b) emission spectra before, during maximum pressure, and after decompression

Figure 6a shows the intensity ratio of these emission lines. It can be seen that the intensity of the line $^5D_0$-$^7F_2$ decreases relative to the intensity $^5D_0$-$^7F_1$ line up to 15 GPa, which indicates an increase in the symmetry environment of Eu^{3+} ions. Also, splitting $^5D_0$-$^7F_1$ line (Figure 6b) shows the increase of the crystal field in the Eu^{3+} surrounding.

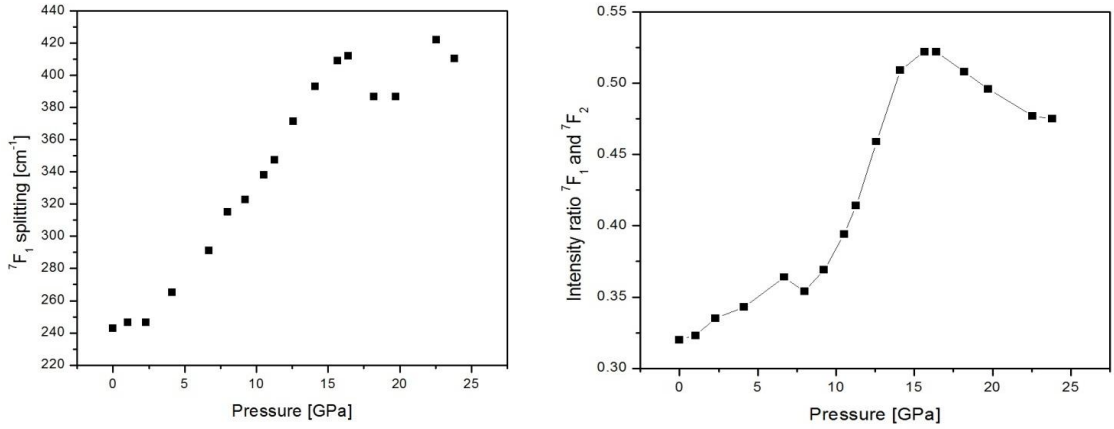

a) b)

Figure 7. Pressure dependence of a) intensity ratio of $^5D_0$-$^7F_1$ magnetic dipole and $^5D_0$-$^7F_2$ electric dipole transitions. b) $^5D_0$-$^7F_1$ emission line splitting.

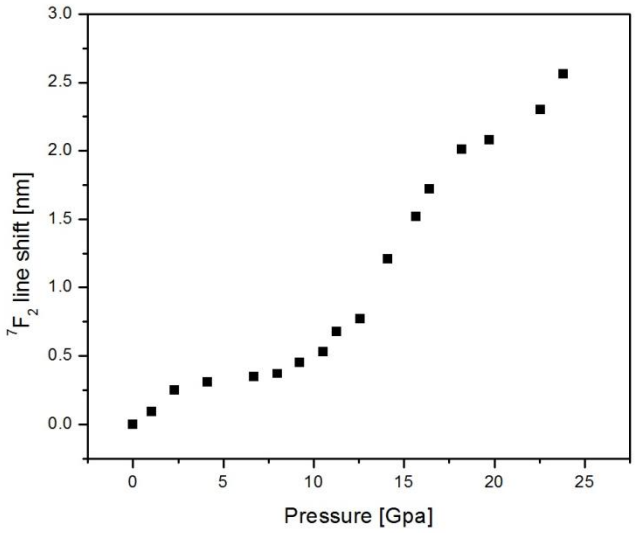

Figure 8. Pressure dependence of $^5D_0$-$^7F_2$ line shift.

4. Conclusion

The effect of doping concentration on photoluminescence properties of Eu^{3+} doped mayenite under high pressure was studied. Pressure dependence of emission spectrum Eu^{3+} doped mayenite shows that it is very sensitive to the local environment around Eu^{3+}, and its intensity depends on the symmetry of the crystal field around the europium ion. Obtained results suggest that $C_{12}A_7$: Eu phosphor may serve as promising red luminescent materials used in the fabrication of optical storage and illumination in dark environments.

Acknowledgments

The authors are grateful to the Ministry of Education, Science, and Technological Development of Serbia for financial support.

References

[1] G. Hentschel, Mayenit, 12CaO·7Al2O3, und Brownmillerit, 2CaO·(Al, Fe)$_2$O$_3$, zwei neue Minerale in den Kalksteineinschlüssen der Lava des Ettringer Bellerberges, Neues Jahrb. Miner. (1964) 22-29.

[2] M. Teusner, R. A. De Souza, H. Krause, S. G. Ebbinghaus, B. Belghoul, M. Martin, Oxygen Diffusion in Mayenite, J. Phys. Chem. C 119 (2015) 9721-9727.

[3] R. Strandbakke, C. Kongshaug, R. Haugsrud, T. Norby, High-Temperature Hydration and Conductivity of Mayenite, $Ca_{12}Al_{14}O_{33}$, J. Phys. Chem. C 113 (2009) 8938-8944.

[4] S. Fujita, K. Suzuki, T. Mori, Y. Lida, Y. Miwa, H. Masuda, S. Shimada, Oxidative Destruction of Hydrocarbons on a New Zeolite-like Crystal of $Ca_{12}Al_{10}Si_4O_{35}$ Including O_2^- and O_2^{2-} Radicals, Chem.Mater. 15 (2003) 255-263.

[5] S. Yang, J.N. Kondo, K. Hayashi, M. Hirano, K. Domen, H. Hosono, Partial oxidation of methane to syngas over promoted C12A7, Appl. Catal. A 277 (2004) 239-246.

[6] C.S. Li, D. Hirabayashi, K. Suzuki, Development of new nickel based catalyst for biomass tar steam reforming producing H2-rich syngas, Fuel Process.Techno. 90 (2009) 790-796.

[7] C.S. Li, D. Hirabayashi, K. Suzki, A crucial role of O_2^- and O_2^{2-} on mayenite structure for biomass tar steam reforming over Ni/$Ca_{12}Al_{14}O_{33}$, Appl.Catal. B: Environ. 88 (2009) 351-360.

[8] S. Kenzi, Application to catalyst of mayenite consisting of ubiquitous elements, Transactions of JWRI, 39 (2010) 281-283.

[9] H. Hosono, N. Asada, Y. Abe, Properrties and mechanism of photochromism in reduced calcium aluminate glasses, J. Apply. Phys. 67 (1990) 2840.

[10] H. Bartl, T. Scheller, Structure of 12CaO.7Al_2O_3, N. Jb. Miner. Mh. 35 (1970) 547–552.

[11] A.N. Christensen, Neutron powder diffraction profile refinement studies on $Ca_{11.3}Al_{14}O_{32.3}$ and CaClO (D.88H.12), Acta. Chem. Scand. 41 (1987) 110–112.

[12] S. Yang, J.N. Kondo, K. Hayashi, M. Hirano, K. Domen, H. Hosono, Formation and desorption of oxygen species in nanoporous crystal 12CaO:7Al_2O_3, Chem. Mater. 16 (2004) 104-110.

[13] K. Kurashige, Y. Toda, S. Matuishi, K. Hayashi, K. Ueda, T. Kamiya, M. Hirano, H. Hosono, Czochralski Growth of 12CaO•7Al_2O_3 Crystals, Cryst. Growth Des. 6 (2006) 1602–1605.

[14] S. Watauchi, I. Tanaka, K. Hayashi, M. Hirano, H. Hosono, Crystal growth of $Ca_{12}Al_{14}O_{33}$ by the floating zone method, J. Cryst. Growth 237 (2002) 801–805.

[15] J.K. Park, T. Shimomura, M. Yamanaka, S. Watauchi, K. Kishio, I. Tanaka, Behavior of oxygen bubbles during crystal growth of $Ca_{12}Al_{14}O_{33}$ by floating method in magnetic field, Cryst. Res. Technol. 40 (2005) 329–333.

[16] K. Sato, S. Yamaguchi, T. Nemizu, S. Fujita, K. Suzuki, T. Mori, Calcium Aluminosilicates as a New Materials with Oxygen Storage Capacity, J. Ceram. Soc. Jpn. 115 (2007) 370-373.

[17] C. Li, D. Hirabayashi, K. Suzuki, Synthesis of higher surface area mayenite by hydrothermal method, Mater. Res. Bull. 46 (2011) 1307–1310.

[18] M.M. Rashad, A.G. Mostafa, D.A. Rayan, Structural and optical properties of nanocrystalline mayenite $Ca_{12}Al_{14}O_{33}$ powders synthesized using a novel route, J. Mater. Sci. Mater. Electron. 27 (2016) 2614–2623.

[19] Branko Matovic, Marija Prekajski, Jelena Pantic, Thomas Bräuniger, Milena Rosic, Dejan Zagorac, Dusan Milivojevic, Synthesis and densification of single-phase Mayenite (C12A7), J. Eur. Ceram. Soc., 36 (2016) 4237-4241.

[20] PDXL Version 2.0.3.0 Integrated X-ray Powder Diffraction Software. Tokyo, Japan: Rigaku Corporation; 2011, p. 196-8666.

[21] Powder Diffraction File, PDF-2 Database and announcement of new database release 2012, International Centre for Diffraction Data (ICDD).